

# Cyclic Voltammetric Behavior of $AB_5$ Metal Hydride Alloys

*B.V. Ratnakumar, S. Di Stefano, S. Suriampudi and (i. Halpert  
Jet Propulsion Laboratory, California Institute of Technology  
4800, Oak Grove Dr., Pasadena, California 91109*

## ABSTRACT

Metal hydride alloys in alkaline Ni-MH rechargeable cells are known to undergo oxidative degradation during charge discharge cycling and especially during overcharge due to a recombination of oxygen diffused from the positive electrode. Such oxidation processes may be accelerated at the positive potentials experienced by the MH electrode during deep- and/or over-discharge. A study of these oxidative processes has been conducted here on various MH alloys by cyclic voltammetry, in the absence of any absorbed hydrogen in the alloys. Also, a qualitative comparative estimation of the stability of these alloys towards oxidation has been made from potentiodynamic measurements.

## 1.0 INTRODUCTION

The ability of certain intermetallic alloys to reversibly absorb significant amounts of hydrogen at low pressures and high potentials is being exploited for several applications. In particular, the replacement of Cd in a Ni-Cd cell with the metal hydride (MH) anodes has resulted in substantial gains in the specific energy, energy density, cycle life and environmental compatibility. Also, the Ni-MH cells have the advantages of sustaining high discharge rates, fast charge rates and gas recombination processes during overcharge and overdischarge similar to Ni-Cd. With the voltage and the charge methods also being almost identical, the Ni-MH cells are expected to gain prominence over Ni-Cd in applications ranging from portable electronic appliances to electric vehicles.

Two classes of metal hydride alloys based on rare earth metals ( $AB_5$ )<sup>(1,2)</sup> and early transition metals ( $AB_2$ )<sup>(3)</sup> are being currently developed at various laboratories. The  $AB_5$  alloys are essentially based on  $LaNi_5$  with various substituents for La as well as Ni to stabilize the alloy against capacity loss during charge-discharge cycling. Hypotheses for these beneficial effects include reduction of the internal stress in the crystalline lattice upon hydrogen absorption and formation of protective surface films. For example, the volume expansion is reduced by a partial substitution of Ni with Co and the interracial properties improved with small amounts of Al or Si<sup>(4)</sup>. Sakai et al<sup>(4)</sup> studied the ternary alloys with different ternary solutes including Mn, Cr, Al, Co and Cu. The cycle life improves upon the substitution of Ni with the ternary solute in the order  $Mn < Ni < Cu < Cr < Al < Co$ . Our recent studies focused on Sn as a ternary solute to  $LaNi_5$ , to provide good cyclic stability and interracial properties, with no penalty on the specific capacity<sup>(5,6)</sup>. A substitution of the rare earth metal site with Ti<sup>(7)</sup>, Zr<sup>(8)</sup>, or other lanthanides such as Nd<sup>(1)</sup> and Ce<sup>(9)</sup> also enhance the cycle life, perhaps because they promote the formation of a protective surface film. This eventually led to the use of relatively inexpensive misch metal, Mm, a naturally occurring mixture of rare earth metals (mainly La, Ce, Pr and Nd) in place of La. The use of misch metal also improved the durability of the alloy, as evident

from the long cycle life as well as the quantitative estimates of the surface layers ( $\text{La}(\text{OH})_3$  and  $\text{Mm}(\text{OH})_3$ ) on the cycled electrodes from X-ray diffraction measurements<sup>(2)</sup>. The alloy formulations currently in use thus contain  $(\text{Mm})(\text{Ni-Co-Mn-Al})_5$  often with other metal additives, such as B and Mo<sup>(10,11)</sup>.

Despite the fact that the effect of the substitution of La with Ce and Nd were studied independently, the optimum composition of the misch metal has not been reported. Nor are the effects of the La substituents on the electrochemical characteristics of the alloy understood. A systematic study was therefore made to vary the misch metal composition, especially with respect to the ratio of La and Ce, and to correlate their electrochemical behavior with the performance in alkaline rechargeable cells. Here, we present the studies related to the oxidative stability of the alloys under extreme positive potentials likely to prevail in the Ni-MH cell under certain conditions of operation,

## 2.0 EXPERIMENTAL

The metal hydride alloys were supplied by Rhone-Poulenc Basic Chemical Co. Out of the several alloys supplied, representative samples were chosen that would vary essentially in the misch metal composition (Table - 1), with the transition metal composition (Ni sites) being approximately similar.

The as supplied alloys were pulverized by ball milling and/or hydrogen absorption - desorption cycles. The MH powder ( $< 75 \mu$ ) was mixed with 20 w% Ni powder (INCO type 255,  $- 1 \mu$ ) and later with 5°A Teflon. Electrodes for the basic electrochemical studies were prepared by filling the cylindrical cavity in the BAS (Bioanalytical Systems) disk electrodes with the mixture of metal hydride electrode powders, of equal quantities in each case. This would ensure equal surface area, charge density ( $\text{mAh/cm}^3$ ) and porosity in all the electrodes, thus permitting a comparison of different MH alloys. NiOOH

electrodes manufactured for an aerospace Ni-Cd cell formed the counter electrode and a Hg/HgO (0.098 V vs. SHE) served as the reference electrode. A three-electrode flooded cell with a Luggin capillary for the reference electrode (Fig. 1 ) was adopted for the basic electrochemical studies. The electrolyte contained 31 w% KOH solution, Potentiodynamic polarization experiments were performed with 273 EG&G Potentiostat/Galvanostat interfaced with an IBM-PC. Cyclic voltammetric studies were carried out with a 173 EG&G Potentiostat/Galvanostat, a 175 EG&G programmer and a Soltech X-Y recorder.

### 3.0 RESULTS AND DISCUSSION

#### 3.1 Cyclic Voltammetry

DC cyclic voltammetry was carried out in the anodic range from the open circuit potential (- 0.65 V vs. Hg/HgO) to 0.4 V vs. Hg/HgO on the virgin alloy, i.e., before incorporating any hydrogen therein. This is expected to provide a comparative assessment of the susceptibility of the alloys towards oxidation. The oxidation of the MH alloy forming a passive surface film is one of the prominent modes of failure of the MH electrodes during charge-discharge cycling(s). Such an oxidation is also responsible for a reduced cycle life in oxygenated environments during overcharge, though the MH alloy is expected to be cathodically protected from oxidation, Further, the voltammetric studies in the electrochemical window of -0.7 to +0.4 V vs. Hg/HgO are relevant to the practical application, i.e., during deep- discharge, especially when the MH electrode becomes capacity-limiting. The potentials experienced by the MH anode in the voltage reversal conditions also fall in the this potential range.

The DC cyclic voltammetric curves of the MH electrodes are illustrated in Fig. 2. The cyclic voltammetric peaks exhibited by different alloys and the corresponding peak heights are listed in (Table -2). The potentials of all the possible reactions in alkaline solutions in

the above potential range (i.e., -0.8 to + 0.5 V vs. Hg/HgO) are listed in (Table-3)<sup>(12)</sup>. A comparison of the **electrode** potentials in Table -3 with the observed peaks in Table-2 reveals that the open-circuit potential of the **MH** alloys is **positive** to the standard potentials for the oxidation of the metallic **constituents** in the alloys, including cobalt and nickel. As such, all the metallic constituents in the alloy would only exist in the oxidized state in the above potential range. This is consistent with the surface studies reported on **AB<sub>2</sub>** alloys that at the surface **all** the alloy elements exist as oxides; only at depths  $\geq 50$  Å **Ni** quickly turns metallic. It is therefore not surprising that the cyclic **voltammetric** curves (**Fig.2**) revealed no peaks corresponding to the oxidation of the alloying elements, e.g., La, Ce, Ni, Co and **Mn**. The oxides thus formed are insoluble in the alkaline solutions and aid in the formation of protective surface films. It may be possible to reversibly reduce the oxide film, especially of cobalt and nickel, during cell charging.

Though the MH alloys do not exhibit any **voltammetric** peaks corresponding to the oxidation of the metals in the potential range of -0.7 to +0.4 V vs. Hg/HgO, it is possible **that** some of the alloying elements may sustain further oxidation to higher valence oxides (Table-3). For example, Mn and Co can transform to trivalent oxides/hydroxides around -0.05 to +0.17 V vs. SHE. Alloys containing Mn, e.g., alloy 6026 and alloy 6039 do exhibit such peaks around - 50 mV, which may be assigned to the formation of **MnO<sub>2</sub>** from Mn(OH)<sub>2</sub>.

Since the observed cyclic **voltammetric** peaks cannot be attributed to the reactions involving electrode elements, they must be related to the reactions involving the electrolyte solution. A comparison of the peak potentials with Table-3 reveals that the observed **voltammetric** peaks are mostly related to oxygen, i.e., to the formation of peroxide ions around 0.245 V vs. SHE and the evolution of oxygen from the peroxide ions at -0.076 V vs. SHE. A **deoxygenation** of the electrolyte does not alter the **voltammograms**, implying that the peaks are related to the hydroxyl ions instead of dissolved oxygen.

All the MH alloys exhibited a strong peak around 0.4 V, which may be attributed to the oxygen evolution from the alkaline electrolyte. Its conjugate reduction peak is also fairly strong in the reverse potential (negative) scan and is dependent on the previous oxidation peak. This implies that the evolution of oxygen or its reduction occurs readily on the MH electrode. This points to a possibility of using the MH electrode as current collector for the oxygen reaction in alkaline media, which maybe exploited in the fields of rechargeable metal - air cells or fuel cells. Another interesting possibility in the above applications would be to a bipolar configuration with the MH biplate functioning both as hydride electrodes on one side and as the oxygen (evolution and/or reduction) electrode on the other side. Surprisingly, alloys containing Mn, e.g., 6026 and 6039 exhibit a weak peak corresponding to the oxygen reduction, though the corresponding oxidation peaks are equally strong as with other alloys. This may be related to the higher manganese oxides formed on these electrodes, as evident from the voltammetric peak at -50 mV vs. SHE.

### 3.2 Potentiodynamic polarization

It is not clear as to what extent the electrolyte-related reactions affect the durability of the MI-1 alloy. In any case, it may be useful to estimate the rates of these reactions. From a Tafel polarization curve, it may be possible to get a comparative estimate of these processes on different alloys. Fig. 3 shows such typical Tafel plots with and without absorbed hydrogen in the alloy. As may be seen from the figure, the reversible potential without absorbed hydrogen is about 300 mV positive (i.e., -650 mV as compared to -950 mV) to the reversible potential with absorbed hydrogen. Also, the current due to the oxidative processes of the electrolyte is at least two orders of magnitude lower than of the hydrogen resorption process. An extrapolation of the Tafel line for the electrolyte processes to the cell operating potentials will provide information on the kinetics of the electrolyte-related processes occurring in the background on the MH electrode, at the cell operating potentials.

Potentiodynamic polarizations were therefore carried out on various MH electrodes containing no absorbed hydrogen in the alloys. The potential was scanned at slow scan rates of 0.5 mV/s to approximate to steady-state conditions. Fig. 4 shows the polarization curves of different MH alloys. These curves do not exhibit a well-defined Tafel behavior. Instead, the curves display passivation-like behavior. It is not clear if this is related to the passivation due to the surface oxide films or to the mass transport effects on the electrolyte-involved reactions. It is therefore difficult to make a quantitative estimate of the kinetics of the reactions involving electrolyte species. Nevertheless, from a qualitative comparison of the polarization, it is clear that the onset of passivation decreases in the order RP 5978 > RP 6025 > IBA MH 5 > RP 6026 > RP6039.

#### 4.0 CONCLUSIONS

The MH alloys in alkaline rechargeable cells are known to undergo oxidative degradation during overcharge. DC cyclic voltammetric studies in the potentials corresponding to deep- and/or over-discharge indicate that in the normal operating range of Ni-MH cell, the alloying elements exist as oxides at the surface and only Mn undergoes further oxidation during deep/over - discharge. On the other hand, some reactions involving electrolyte species, i.e., formation of peroxide ions and their subsequent oxidation are evident from the cyclic voltammetry. The MH alloy electrode sustain both oxygen evolution and its conjugate reduction readily, making them a likely electrode materials for oxygen reaction in electrochemical devices such as metal (or MH) -air cells or fuel cells. It is, however, not possible to study the corrosion processes on the MH alloys by either cyclic voltammetry or polarizations studies.

## 5.0 ACKNOWLEDGMENT'S

This work was carried out at the Jet Propulsion Laboratory, California Institute of Technology under contract with the National Aeronautics and Space Administration. Gratitude is extended to Dr. Bao-Min Ma of Rhone Poulenc Basic Chemical Co., for providing the MH alloys. Part of this work was carried out under funding by the DOE grant DE-FG03-94ER14493.

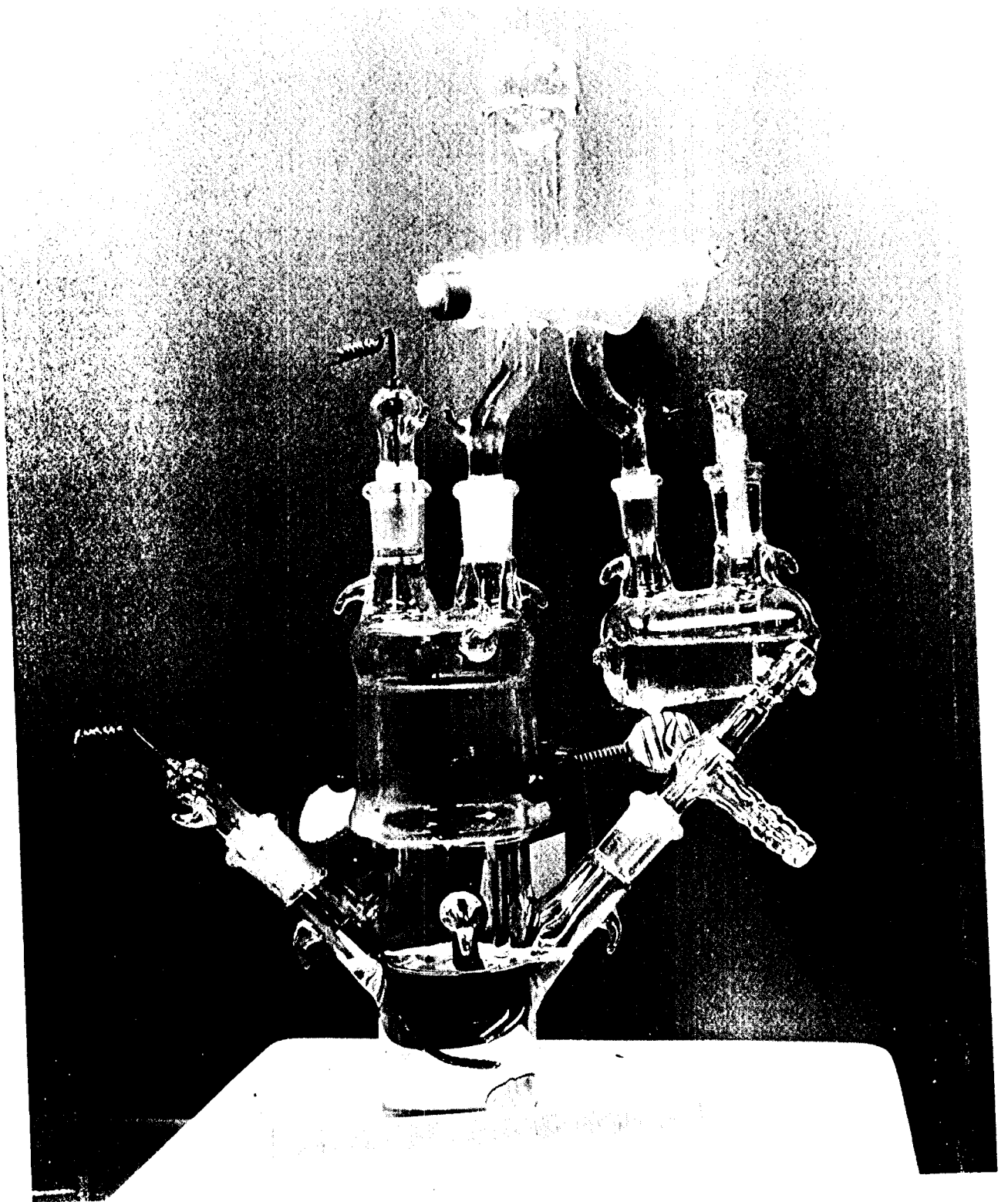
## 6.0 REFERENCES

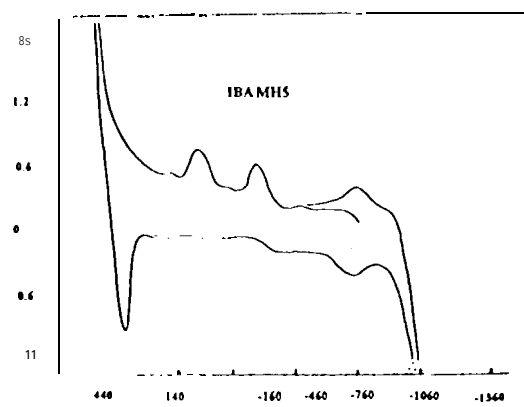
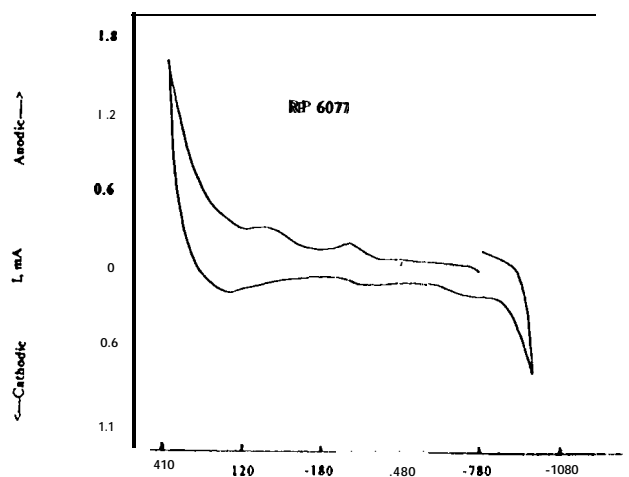
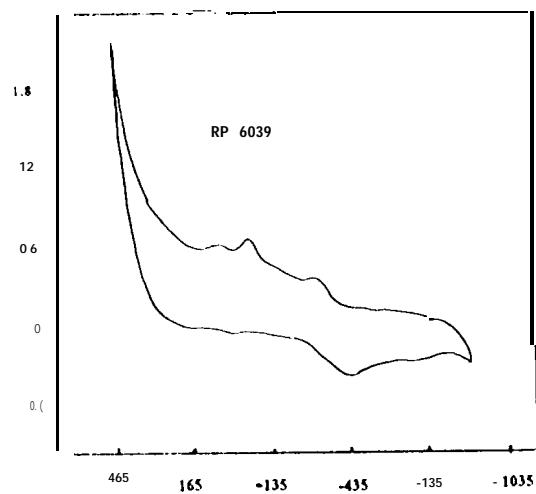
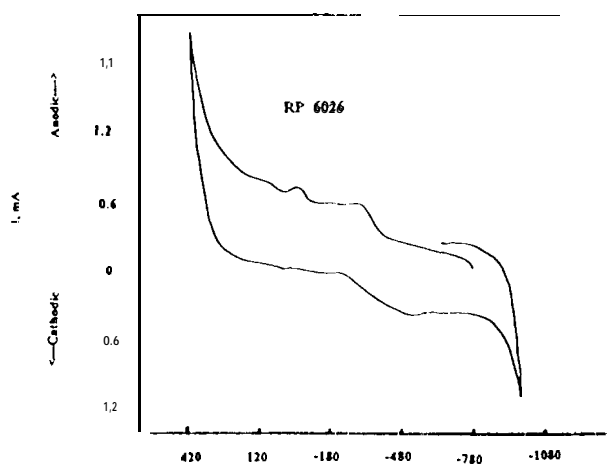
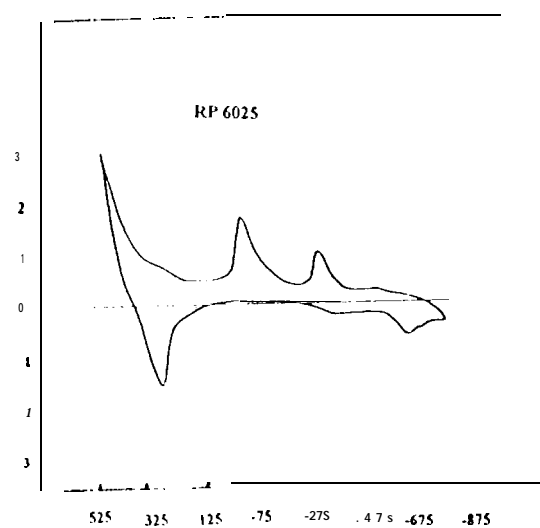
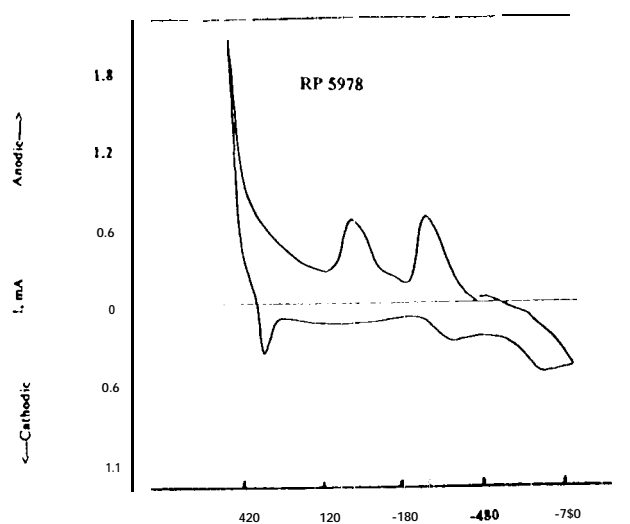
1. J. G. G. Willems, *Philips J. Res.*, **39** (Suppl. 1), 1 (1984); J. J.G. Willems and K. H. J. Buschow, *J. Less Common Metals*, **129**, 13 (1987).
2. T. Sakai, K. Muta, H. Miyamura, N. Kuriyama and H. Ishikawa, *Proc. Symp. Hydrogen Storage Materials : Batteries and Electrochem.*, ECS Proc. Vol. 92-5, p. 59 (1992); T. Sakai, H. Yoshinaga, H. Miyamura and H. Ishikawa, *J. Alloys and Compounds*, **180**, 37 (1992).
3. S. R. Ovshinsky, M. A. Fetcenko and J. Ross, *Science*, **260**, 176 (1993); M. A. Fetcenko, S. Venkatesan and S. R. Ovshinsky, *Proc. Symp. Hydrogen Storage Materials : Batteries and Electrochemistry*, ECS Proc. Vol. 92-5, p. 141 (1992); M. A. Fetcenko, S. Venkatesan, K. C. Hong and B. Reichman, *Power Sources*, Vol. 12, p. 411 (1988).
4. T. Sakai, K. Oguru, H. Miyamura, N. Kuriyama, A. Kato and H. Ishikawa, *J. Less-Common Metals*, **161**, 193 (1990).
5. B. V. Ratnakumar, G. Halpert, C. Witham and B. Fultz, *J. Electrochemical Soc.*, **141**, 189 (1994).
6. B. V. Ratnakumar, S. Surampudi, S. DiStefano, G. Halpert, C. Witham and B. Fultz, *Proc. Symp. Hydrogen Batteries, ECS Fall Meeting*, Miami Beach, FL, Oct. (1994).
7. T. Sakai, H. Miyamura, N. Kuriyama, A. Kato, K. Oguru and H. Ishikawa, *J. Less-Common Metals*, **159**, 127 (1990).

8. T. Sakai, H. Miyamura, N. Kuriyama, A. Kate, K. Oguru and H. Ishikawa, *J. Electrochem. Soc.*, 137, 795 (1990).
9. T. Sakai, T. Hazama, H. Miyamura, N. Kuriyama, A. Kato and H. Ishikawa, *J. Less-Common Metals*, 172-174, 1175 (1991).
10. N. Furukawa, 'Sanyo's Metal Hydride Cells', *Proc. IBA Meeting*, Seattle, WA, Ott. 12-13 (1990); M. Tadokoro, M. Naogami, Y. Chikano, M. Kimoto, T. Ise, K. Nishio and N. Furukawa, *J. Alloys and Compounds*, 197, 179 (1993).
11. I. Matsumoto and A. Ohta (Matsushita, Japan), *Proc. IBA Meeting*, Seattle, WA, Ott. 12-13 (1990),
12. A. J. de Bethune and N. A. Swendeman Loud, "Standard Aqueous Electrode Potentials and Temperature Coefficients at 25° C", Clifford A. Hampel, Skokie, IL.

## 7.0 FIGURE CAPTIONS

- Fig. 1: Electrochemical cell for the DC cyclic voltammetric and polarization measurements on MH alloy disc electrodes in 31 w% KOH solution.
- Fig. 2: DC Cyclic voltammetric curves of various MH alloy electrode at 5 mV/s.
- Fig. 3: Typical Tafel polarization curves of MH alloy electrode in 31 w% KOH solution 1) without and 2) with absorbed hydrogen.
- Fig. 4: Potentiodynamic polarization curves of MH disc electrodes containing 1) RP 5978, 2) RP 6025, 3) IBA MH 5, 4) RP 6026 and 5) RP 6039 alloys at a scan rate of 0.5 mV/s, during oxidation and before hydrogen absorption.
- Table-1: Composition of various MH alloys supplied by Rhone-Poulenc, Inc.
- Table-2: Observed voltammetric peaks of MH alloys due to various electrochemical reactions.
- Table-3: Electrode potentials of possible reactions at the MH electrode in alkaline solutions in the potential range of -0.8 to +0.5 V vs. SHE.





$E, \text{mV vs. Hg/HgO}$

$E, \text{mV vs. Hg/HgO}$

Fig. 2

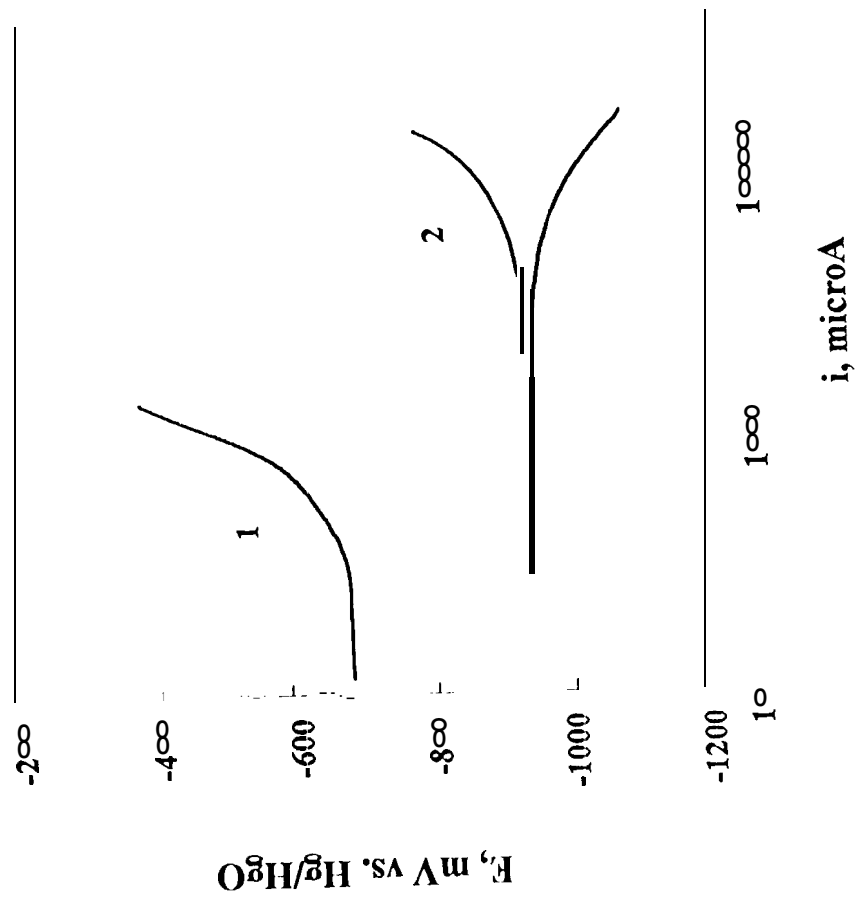


Fig 3

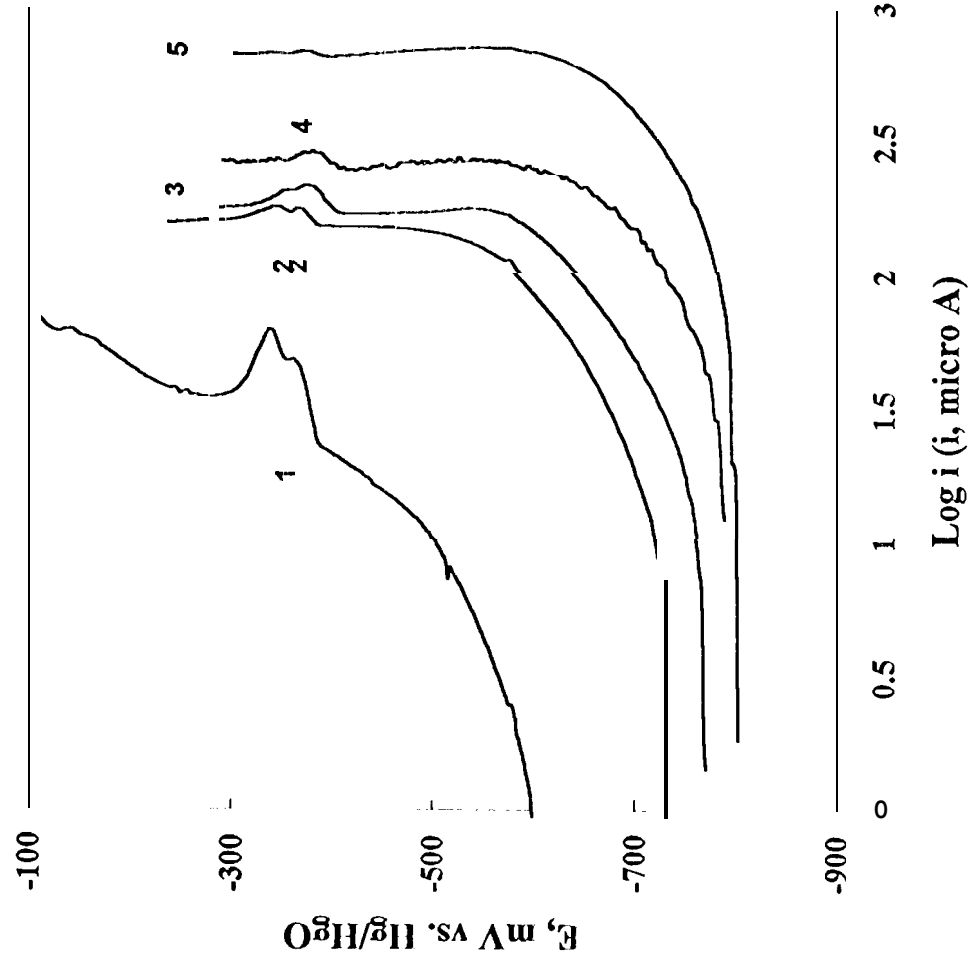


Fig. 4.

COMPOSITION (mol %)								
ALLOY #	La	Ce	Nd	Pr	Ni	Co	Mn	Al
5978	1	0	0	0	4.96	0	0	0
6025	0.3	0.51	0.07	0.13	3.56	0.76	0.4	0.3
6026	0.25	0.55	0.07	0.13	3.68	0.75	0.4	0.34
6039	0.64	0.25	0.04	0.08	3.51	0.77	0.4	0.31
6077	0.49	0.2	0.09	0.22	3.05	1.5	0	0.53

Table 1

Proc	Assigned Electrochemical Reaction	5978		6025		6026		6039		6077		IBA 5	
		E, mV	I <sub>p</sub> , mA	E, mV	I <sub>p</sub> , mA	E, mV	I <sub>p</sub> , mA	E, mV	I <sub>p</sub> , mA	E, mV	I <sub>p</sub> , mA	E, mV	I <sub>p</sub> , mA
Oxid	$(\text{OH})_{\text{aq}} + 2\text{OH}^- = \text{HO}_2^- + \text{H}_2\text{O} + 2e^-$	-330	0.68	-390	1.0	-375	0.56	-370	0.875	-345	0.24	-275	0.58
	$\text{HO}_2^- + \text{OH}^- = \text{O}_2 + \text{H}_2\text{O} + 2e^-$	-80	0.66	-95	1.65	-115	0.72	-120	1.1	-45	0.35	-70	0.72
	$\text{Mn}(\text{OH})_2 + 2\text{OH}^- = \text{MnO}_2 + 2\text{H}_2\text{O} + 2e^-$	---	---	---	---	-5	~0.2	-10	1.0	---	---	---	---
	$4(\text{OH})^- = \text{O}_2 + 2\text{H}_2\text{O} + 4e^-$	385	2.06	420	2.0	335	2.06	390	5.5	315	1.66	385	2.4
	$\text{O}_2 + 2\text{H}_2\text{O} + 4e^- = 4(\text{OH})^-$	377	0.38	215	1.6	---	---	---	---	105	0.16	275	0.98
Red	$\text{MnO}_2 + 2\text{H}_2\text{O} + 2e^- = \text{Mn}(\text{OH})_2 + 2\text{OH}^-$	---	---	---	---	---	---	-50	0.2	---	---	---	---
	$\text{HO}_2^- + \text{H}_2\text{O} + e^- = (\text{OH})_{\text{aq}} + 2\text{OH}^-$	-415	0.26	-360	0.25	---	---	-500	1.05	-415	0.1	-425	0.24
	$\text{Ni (or Co)}_2(\text{OH})_2 + 2e^- = \text{Ni} + 2\text{OH}^-$	-735	0.52	-720	0.65	---	---	-750	0.3	-815	0.195	-790	0.46

Table 2

E vs. SHE	Metal	Reaction
-2.84 to -2.90 V	La, Ce, Nd, Pr	$M + 3 (OH)^- = M(OH)_3 + 3 e^-$
-0.72 V	Ni	$Ni + 2 (OH)^- = Ni(OH)_2 + 2 e^-$
-0.73 V	Co	$Co + 2 (OH)^- = Co(OH)_2 + 2 e^-$
0.17 V		$Co(OH)_2 + (OH)^- = Co(OH)_3 + e^-$
-1.55 V	Mn	$Mn + 2 (OH)^- = Mn(OH)_2 + 2 e^-$
-0.05 V		$Mn(OH)_2 + 2 (OH)^- = MnO_2 + 2 H_2O + 2 e^-$
0.15 V		$Mn(OH)_2 + (OH)^- = Mn(OH)_3 + e^-$
-2.3 V	Al	$Al + 3 (OH)^- = Al(OH)_3 + 3 e^-$
-0.245 V	Oxygen	$(OH)_{aq} + OH^- = HO_2^- + H_2O + e^-$
-0.076 V		$HO_2^- + (OH)^- = O_2 + H_2O + 2 e^-$
0.40 V		$4 OH^- = O_2 + 2 H_2O + 2 e^-$
-0.828 V	Hydrogen	$H_2 + 2 OH^- = 2 H_2O + 2 e^-$

Table-3